Mai Thi TRINH[1,2]
Dac Trung NGUYEN[2]
Tuan Quoc PHAM[2]
Anh Ngoc PHAM[3]
Van Duy DINH[2*]

HYDRO-FORMING A CROSS-SHAPED COMPONENT FROM TUBE BILLET

This paper investigates the tube hydroforming (THF) process through numerical simulations conducted in Abaqus/CAE software, aiming to identify optimal technological parameters for cross-shaped forming from seamless tube billets. The study focuses on seamless copper CDA110 tube billets as the primary material. The simulation evaluates critical factors such as thinning, thickening, and the height of the formed bulge. Output data is collected and analysed using linear regression methods, followed by a comparison with technical requirements to assess suitability. The research results provide both scientific and practical foundations, contributing to the optimization of the cross-shaped hydroforming process while expanding the applicability of this technology in industrial production.

1. INTRODUCTION

Tube hydroforming (THF), a well-established technology since the 1990s [1], is particularly effective for shaping complex components with high precision, such as automotive frames and aerospace load-bearing structures [2, 3]. This advanced method utilizes high-pressure fluid to shape metal components, significantly reducing waste and eliminating intermediate operations [3].

Compared to traditional methods such as machining, welding, and laser cutting, THF offers exceptional advantages in sustainability and manufacturing efficiency [4, 5]. It not only enhances the mechanical properties of products but also enables the formation of complex shapes such as automotive frames, load-bearing components in aviation, and medical applications [6, 7].

_____

[1] University of Economics – Technology for Industries, 456 Minh Khai, Vinh Tuy Ward, Hai Ba Trung District, Hanoi, Vietnam.
[2] Hanoi University of Science and Technology, 1 Dai Co Viet, Bach Khoa ward, Hai Ba Trung district, Hanoi, Vietnam.
[3] School of Mechanical Engineering, Vietnam Martime University, Hai Phong, Vietnam
[*] E-mail: duy.dinhvan@hust.edu.vn

Numerous studies have examined aspects of THF, such as formability [8, 9], the role of axial feeding in minimizing deformation [10], and optimization of fluid pressure to enhance product quality [11]. For instance, Satish et al. evaluated the effectiveness of THF in micro-scale applications, emphasizing the importance of parameters such as friction and fluid pressure [12]. Other research has suggested elastic deformation adjustments to dies to enhance dimensional accuracy [13] or analysed deformation characteristics during the forming of T- and cross-shaped components [14].

However, the optimal range of fluid pressure (P_i) and axial punch displacement (A_i) for cross-shaped components formed from seamless tube billets has not been thoroughly investigated. As highlighted by Bogoyavlensky et al., incorrect choices of pressure or feed can lead to tearing or wrinkling during the forming process [15]. Moreover, current studies lack experimental data to validate numerical simulations, particularly for cross-shaped components with high mechanical property requirements.

To bridge this gap, this study conducted numerical simulations of the hydroforming process for cross-shaped components made from seamless copper CDA110 tubes using Abaqus/CAE. The research focused on evaluating key parameters such as thinning, thickening, and boss height, thereby developing regression equations and determining optimal ranges. These findings aim to expand the practical applications of THF in industrial manufacturing.

2. RESEARCH OBJECT

2. 1. MATERIAL AND BILLET SHAPE

The component is formed from a seamless tube billet with a diameter of 22.22 mm, made of annealed copper CDA110. The initial parameters of the tube billet are shown in Fig. 1, while the material properties are detailed in Table 1 [1]. The desired product shape is illustrated in Fig. 2.
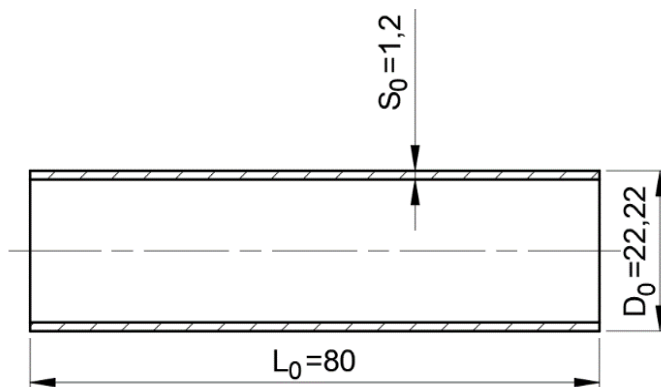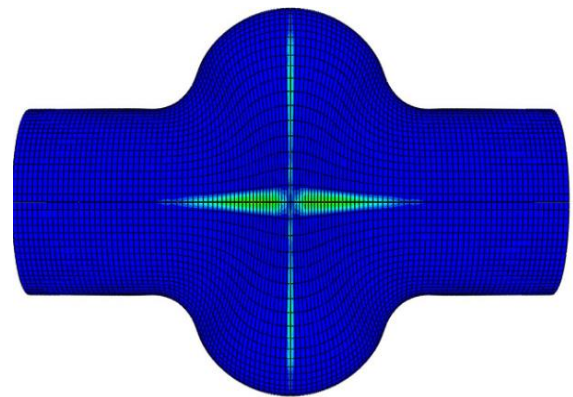

Fig. 1. Geometric specifications of the billet

Fig 2. Shape of the formed component

Table 1. Technical specifications of annealed Cu CDA110 material [1]

Parameters and technical characteristics of CDA110 material	Value
Material parameter surveying temperature (°C)	24
Density, ρ (kg/m^3)	8940
Elastic modulus, E (GPa)	115
Material constants, C (MPa)	325
Endurance limit exponent, n	0.54
Poisson's ratio, v	0.33
Yield strength, σ_y (MPa)	170
Tensile strength, σ_u (MPa)	370
Relative elongation, $\mathcal{E}$ (%)	40

2.2. MODELING THE HYDROFORMING PROCESS IN ABAQUS/CAE

The simulation was conducted using Abaqus/CAE, selected for its accuracy in modeling deformation and stress distribution. Its advanced tools enabled efficient analysis of the hydroforming process for seamless copper CDA110 tube billets. The tube billet is modeled in Abaqus/CAE with the following main geometric parameters:
- Outer diameter of the tube: $D_0 = 22.22$ mm
- Initial length of the billet: $L_0 = 80$ mm
- Tube wall thickness: $S_0 = 1.2$ mm.

The protrusion to form the cross shape has a diameter equal to D_0, measured as 22.22 mm, while the height of the cross shape is determined freely during the forming process. The forming die has basic specifications as shown in Fig. 3.

Fig 3. Basic specifications of the die

To optimize the modeling process and reduce computation time in Abaqus, the study only builds 1/8 of the component model, as shown in Fig .4. The remaining part is completed by applying symmetry along the planes, reconstructing the final shape of the component without the need to simulate the entire model.
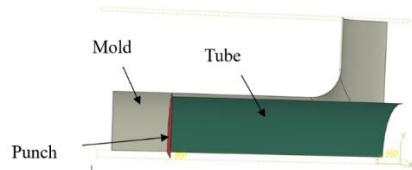

Fig 4. Geometric assembly model constructed in Abaqus

Meshing Process for the Model

After completing the model construction, the billet is meshed to generate finite elements. The finite element model was developed in Abaqus/CAE, employing S4R shell elements with a mesh size of 0.5 mm × 0.5 mm to ensure accurate deformation simulation (Fig. 5).
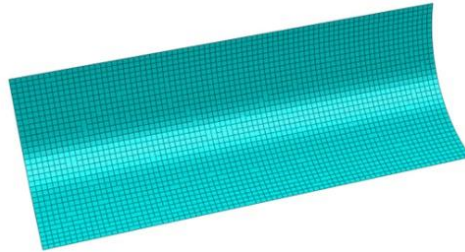

Fig 5. Tube element mesh model

2.2.1. BOUNDARY CONDITION SETUP

Throughout the simulation, the tube billet and its components interact under a constant friction coefficient of 0.1 across the entire structure. The die and punch are modeled as perfectly rigid, with the die remaining completely fixed during the process. The punch is programmed to move axially along the billet with displacement values of 10 mm, 14 mm, and 18 mm, respectively [16].

The internal fluid pressure Pi within the tube is determined based on calculations from single-load impact [15] and combined loading [1]. The range of forming pressures is varied corresponding to values of 25 MPa, 30 MPa, 35 MPa, 40 MPa, 45 MPa, and 50 Mpa [16]. For liquid pressure values outside the investigated range, additional studies were conducted. However, the resulting protrusion heights were either too low or the thinning was excessively large. Therefore, the data from these cases were excluded from the analysis. The outer surfaces of the billet are constrained to prevent undesired displacements along the axes, while symmetry planes are appropriately established to reduce the computational model size.

2.2.2. SIMULATION SETUP

The simulation was conducted with an assumed constant friction coefficient of 0.1, under the combined loading of internal liquid pressure and axial feeding by the punch. The application of internal fluid pressure P_i and the axial displacement of the punch A_i are time-dependent, with their ratios fixed as shown in Table 2.

2.2.3. RESULTS COLLECTION AND DATA EVALUATION

After modeling and simulating the hydroforming process for the tube billet to create a cross-shaped component, the resulting product image is shown in Fig. 6.

The collected data include the height of the formed bulge, the thinning value at the most expanded region of the bulge, and the thickening value at the transition zone (Fig. 6). These

data are compared and analysed to clarify the role of internal fluid pressure within the tube and the axial feed displacement of the punch on forming quality.

Table 2. Data Table of Forming Pressure Application and Data Table of Axial Feeding Application Over Time

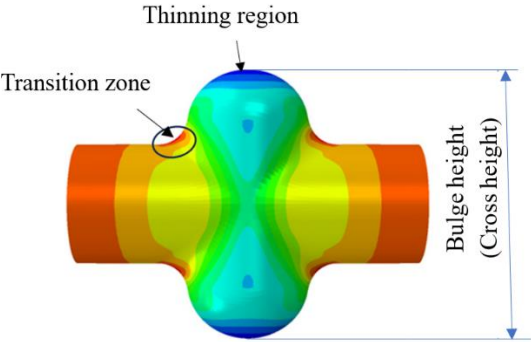| Data Table of Forming Pressure Application	Data Table of Axial Feeding Application Over Time

Fig 6. Image of the component formed after simulation & Data collection regions

2.3. RESULTS AND DISCUSSION

2.3.1. COLLECTING RESULTS FROM ABAQUS SIMULATION

Simulations were conducted with varying input parameters, including internal fluid pressure within the tube (Pi) and axial feed displacement (Ai), as described above. The results obtained from the simulation were measured and compiled in Table 3. From the collected data, component images, and the stress-strain relationship charts, the following observations can be made:
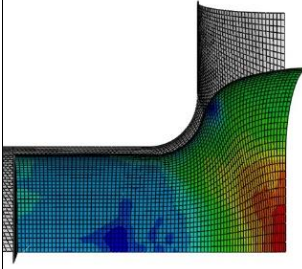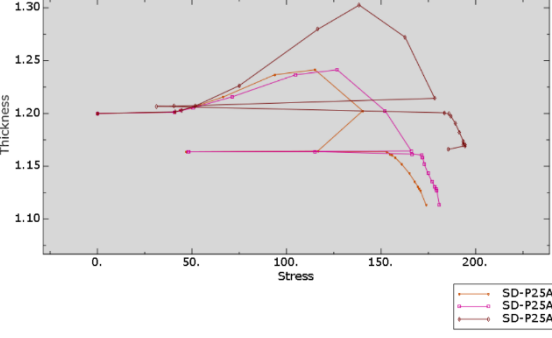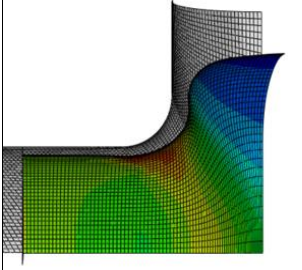
The simulations were performed with varying input parameters, including internal fluid pressure (P_i) and axial punch displacement (A_i), as described earlier. The results obtained from the simulation were measured and summarized in Table 3. The key collected data included the thinning value at the farthest bulging region, the thickening value at the transition region, and the height of the boss. These values were analysed to clarify the roles of fluid pressure inside the tube and the axial punch feed in determining the quality of the formed product.

Table 3. Summary of results from the tube hydroforming simulation performed in Abaqus/CAE

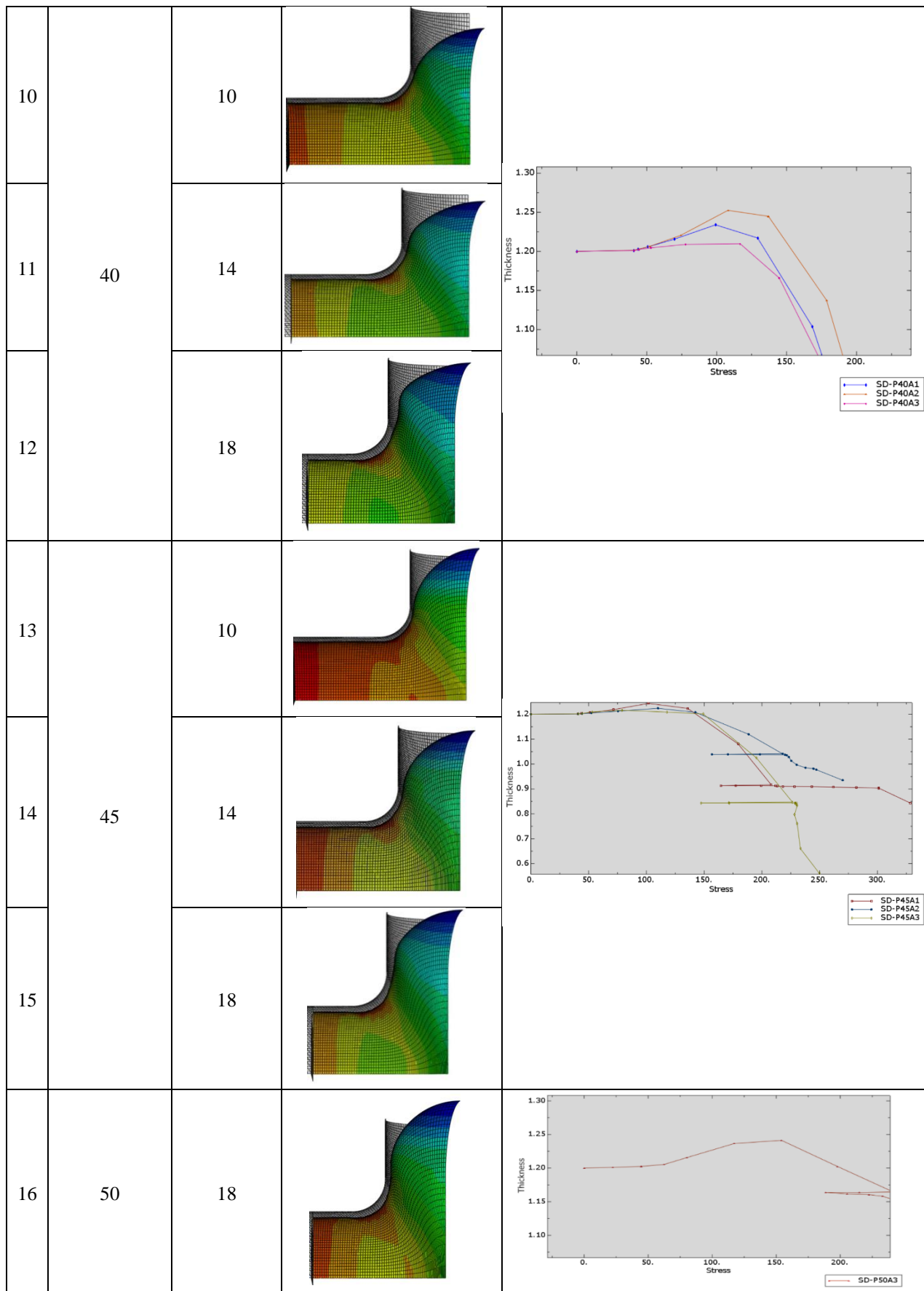| SN	Internal fluid pressure within the tube P_i (Mpa)	Axial feed displacement A_i (mm)	Thinning value B_i (mm)	Cross height H_i (mm)	Thickening value (N_i mm) (Use approximate data)
1	25		1.113	38.42	1.618
2	30		1.033	40.22	1.628
3	35	10(A_1)	0.935	42.22	1.608
4	40		0.803	44.42	1.574
5	45		0.402	51.42	1.533
6	25		1.148	41.02	1.739
7	30		1.077	43.02	1.777
8	35	14(A_2)	0.935	42.22	1.608
9	40		0.89	46.82	1.780
10	45		0.725	49.82	1.723
11	25		1.166	44.22	1.926
12	30		1.102	45.62	1.921
13	35		1.027	48.22	1.961
14	40	18(A_3)	0.950	49.82	1.985
15	45		0.843	51.82	1.968
16	50		0.561	56.42	1.942

The simulation results generated using Abaqus/CAE are presented in Table 4.

Table 4. Collected component images and stress-thinning relationship charts from the simulation

SN	Internal fluid pressure with As fluid pressure increases in the tube P_i (MPa)	Axial feed displacement A_i (mm)	Component images after simulation	Stress-thinning relationship chart
1	25	10		
2		14		

3		18		
4		10		
5	30	14		
6		18		
7		10		
8	35	14		
9		18		

10		10		
11	40	14		
12		18		
13		10		
14	45	14		
15		18		
16	50	18		

From Table 3, the relationships between P_i, A_i, and the output parameters can be observed. As the fluid pressure increases, the thinning becomes more pronounced, particularly in regions subjected to high tensile stresses. Conversely, a well-matched axial punch feed improves thinning control, ensuring the product's dimensional integrity.

In contrast, excessive fluid pressure without adequate axial punch feed can lead to severe thinning, potentially surpassing acceptable limits, which may cause product defects. Similarly, overly rapid or mismatched axial punch feed can result in incomplete die contact, leading to shape inaccuracies or decreased product quality.

The insights from this analysis highlight the critical importance of synchronizing fluid pressure and axial punch feed during the hydroforming process. Furthermore, the diagrams and images presented in Table 4 reinforce these findings, providing visual confirmation of the simulation's accuracy and the reliability of the regression equations developed.

From the stress-strain relationship chart, it can be observed that as stress increases, the strain may remain unaffected in some cases, while in others, a slight increase in stress can result in significant strain (Table 4). This indicates a nonlinear relationship between stress and strain during the tube hydroforming process.

2.3.2. DEVELOPING LINEAR REGRESSION EQUATIONS

The research team used input and output data from Table 3 to develop linear regression equations:

a) Regression Equation for the Thinning Variable *Bi*

- For axial displacement A1=10 mm, Fluid pressure Pi values are 25, 30, 35, 40, and 45 MPa: $B1 = -0.03304Pi + 2.0136$

- For axial displacement A2=14 mm, Fluid pressure Pi values are 25, 30, 35, 40, and 45 MPa: $B2 = -0.02066Pi + 1.6781$

- For axial displacement A3=18 mm, Fluid pressure Pi values are 25, 30, 35, 40, 45, and 50 MPa: $B3 = -0.02232Pi + 1.777$

Table 5. Reliability data of the regression equation for the thinning variable

Measurement Indices	A_1	A_2	A_3
MAE	0.07976	0.0228	0.0528
RMSE	0.08902	0.02429	0.06043
R-squared	0.8732	0.9731	0.9087

Table 5 demonstrates that the evaluation indices of the regression equation for the thinning variable achieve a good level of fit. Specifically: The *MAE* and *RMSE* indices are both below 10%, the *R-Squared* index reflects very high reliability, exceeding 87.32%. These results confirm that the range of axial feed displacement A_i and fluid pressure P_i in the surveyed region can be reliably applied in practical production.

Based on this, and with the requirement that the thinning should not exceed 30% to avoid tearing during processing, the following conditions are established:

- For A_1: $0.36 \leq -0.03304P_i + 2.0136$ $=> P_i \leq 50.06$ MPa
- For A_2: $0.36 \leq -0.02066P_i + 1.6781$ $=> P_i \leq 63.81$ MPa
- For A_3: $0.36 \leq -0.02232P_i + 1.777$ $=> P_i \leq 63.50$ MPa.

Thus, to ensure that thinning does not exceed 30%, the pressure P_i should not exceed the following values for each axial punch displacement:

For axial displacement A_1: $P_i \leq 50.06$ MPa
For axial displacement A_2: $P_i \leq 63.81$ MPa
For axial displacement A_3: $P_i \leq 63.50$ MPa

b) Regression Equation of Thickness Variable N:

For the punch displacement range A_1: $N_1 = -0.00448P_i + 1.749$
For the punch displacement range A_2: $N_2 = -0.00058P_i + 1.7457$
For the punch displacement range A_3: $N_3 = 0.0014P_i + 1.898$

Table 6. Reliability Data of the Regression Equation for the Thickness Variable

Measurement Indices	A_1	A_2	A_3
MAE	0.01336	0.04696	0.01733
RMSE	0.01425	0.0625	0.01954
R-squared	0.8317	0.0043	0.2723

Table 6 shows that only the axial feeding value A_1 achieves an acceptable reliability of 83.17%, while the feeding values A_2 and A_3 have very low reliability, below 30%. Therefore, these two feeding values can be excluded if the requirement is to ensure that the thickness of the product meets high standards.

To determine the internal fluid pressure P_i that ensures the tube thickness does not exceed the range from 1.2 mm to 1.56 mm, we only need to focus on the experimental domain of A_1. In that case:

$$1.2 \leq N1 = -0.00448P_i + 1.749 \leq 1.56$$
$$\text{So: } 42.19 \text{ MPa} \leq P_i \leq 122.54 \text{ MPa}$$

c) Regression Equation of Cross-Section Height H_i:

Axial displacement of the punch A_1: $H_1 = 0.604P_i + 22.20$
Axial displacement of the punch A_2: $H_2 = 0.428P_i + 29.60$
Axial displacement of the punch A_3: $H_3 = 0.464P_i + 31.95$

Table 7. Reliability Data of the Regression Equation for Cross-Section Height

Measurement Indices	A_1	A_2	A_3
MAE	1.264	0.944	0.653
RMSE	1.445	1.213	0.777
R-squared	0.8973	0.8616	0.9630

2.3.3. VALIDATION OF THE REGRESSION EQUATIONS

Choose the forming fluid pressure value within the recommended range ($Pi = 48$ MPa), applied with the axial displacement of the punch $A1 = 10$ mm. The results calculated for the

thin variable *B1* = 0.428 mm and the thick variable *N1* = 1.534 mm. These values confirm the accuracy of the conclusions stated above.
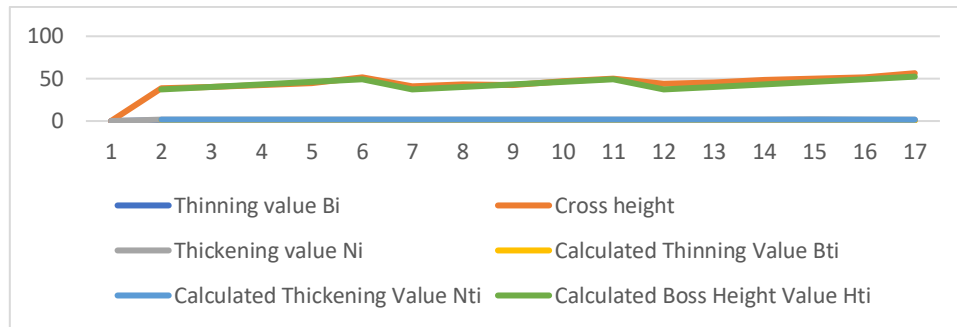

Fig. 10. Reliability Test Chart of the Linear Regression Equation

From the chart, it can be *observed that the values for the thin variable Bi, thick variable Ni, and cross-section height Hi*, measured from the Abaqus software, closely match the values calculated from the regression equations. This correlation aligns with the reliability indicators presented in Tables 5, 6, and 7.

3. CONCLUSION

This study focused on simulating and analyzing the hydroforming process (HP) of cross-shaped parts from seamless copper CDA110 tube billets using Abaqus/CAE software. The research results led to several important conclusions as follows:

Determination of Optimal Parameter Range: The study establisher an appropriate range for the forming fluid pressure (42.2 MPa$\leq Pi \leq$ 50.6 MPa) and axial punch displacement (A_i = 10 mm), ensuring product quality, with the thin and thick variables not exceeding 30%.

Regression Equation and Reliability:

The linear regression equation for cross-section height achieved high reliability, with small coefficients and a confidence level exceeding 89%, proving the compatibility between the predicted results and experimental data.

Role of Pressure and Feeding: The simultaneous relationship between internal fluid pressure (Pi) and axial displacement (A$_i$) plays a crucial role in ensuring product quality and shape after forming. Accurate control of axial feeding and pressure over time is a key factor that requires further investigation to optimize the production process.

Practical Application: The specific value range determined for seamless tube billets (diameter 22.22 mm, thickness 1.2 mm, length 80 mm) serves as a crucial basis for experimental application, contributing to filling the data gap in areas where current studies have not fully published. The research provides a foundation for establishing appropriate process parameters and optimizing the production of complex parts using hydroforming technology.

Proposed Future Research Directions:

Optimal Feeding Level: With fixed forming pressure, there exists an optimal axial feeding range to ensure product quality. Too low feeding can lead to excessive thinning, while too high feeding may cause localized thickening or geometric defects.

Development of Research: Combining real-world experiments with simulations to extend the application scope to other materials and more complex billet shapes.

This study provides a foundation for establishing appropriate process parameters, thereby optimizing the manufacturing of complex components using tube hydroforming technology. Although the current work is limited to numerical simulation, numerous studies have shown that the deviation between simulation results and experimental data typically ranges from 1.5% to less than 5% [17–19]. While these studies do not directly focus on tube hydroforming, they offer a reliable reference that supports the applicability and accuracy of numerical simulation methods in research and experimentation.

REFERENCES

[1] PHAM N.V., 2006, *Hydraulic Stamping Technology*, Hanoi University of Science and Technology.
[2] ASNAFI N., 1999, *Analytical Modelling of Tube Hydroforming*, Thin-Walled Structures, 34, 295–330.
[3] ABRANTES J.P., et al., 2005, *Experimental and Numerical Simulation of Tube Hydroforming*, Journal of Materials Processing Technology.
[4] KIM S.-W., et al., 2009, *Bursting Failure Prediction in Tube Hydroforming*, Int. J. Adv. Manuf. Technol.
[5] KANT R., 2011, *Effect of Die Entrance Radius on Tube Formability*, Applied Science & Technology Research Excellence.
[6] KADKHODAYAN M., et al., 2015, *Optimization of T-shape Hydroforming*, Metal Forming.
[7] SATISH., et al., 2024, *Review of Emerging Hydroforming Technologies: Micro Applications*, Advanced Materials Research.
[8] PAUNOIU V., et al., 2023, *Dimensional Accuracy Enhancement in Hydroforming*, Journal of Modern Manufacturing Technologies.
[9] ABRANTES J.P., 2023, *Improvement of Formability in Parallel Double-Branched Tube Hydroforming*, Journal of Materials Processing Technology.
[10] KADKHODAYAN M., et al., 2020, *Material Deformation Behavior in T-Shape Hydroforming*, SN Applied Sciences.
[11] KANT R., et al., 2021, *Finite Element Analysis in Hydroforming*, Applied Mechanics Reviews.
[12] VU D.Q., NGUYEN D.T., et al., 2024, *Study on the Effect of Internal Pressure and Axial Feed in Tube Hydrostatic Forming Process of T-shaped Joints*, Springer Nature, https://doi.org/10.1007/978-3-031-39090-6_44.
[13] KADKHODAYAN M., 2010, *Loading Path Optimization in Hydroforming*, Metal Forming.
[14] SIMULIA, 2016, Abaqus Documentation, http://130.149.89.49:2080 › index.html.
[15] BOGOYAVLENSKY., et al., 1988, *Hydro-plastic Processing of Metals*, Mashinostroenie, Moscow; Teknika, Sophia.
[16] TRINH M.T., DINH D.V., et al., 2025, *Hydro-Forming of U-Shaped Parts with Branches*, Engineering technology & Applied sciense research, https://doi.org/10.48084/etasr.9227.
[17] TRIEU Q.-H., LUYEN T.T., NGUYEN D.-T., 2024, *Optimization and Modelling of Fracture Height in SECC Cylindrical Cup Deep Drawing Processes*, Journal of Machine Engineering, 24/1, 74–86, https://doi.org/10.36897/jme/185476.
[18] ABDULLAH E., JALIL A., 2025, *Enhancing Experimental Prediction of Springback in Forming Processes Using Advanced Finite Element Modelling*, Journal of Machine Engineering, 25/1, 79–101, https://doi.org/10.36897/jme/202916.
[19] MAJSTOROVIC V.D., et al., 2023, *Towards the Digital Model of Tool Lifecycle Management in Sheet Metal Forming*, Journal of Machine Engineering, 23/3, 141–166, https://doi.org/10.36897/jme/171664.